

Tightly-Coupled Integration of Inertial and Magneto-Inductive Sensors for Large-Scale Indoor Localization

Changhao Chen, Andrew Markham, Niki Trigoni

Abstract—Indoor localization and navigation problem has long received much attention from both academics and industries, due to its importance in many applications, such as location-based services, logistics, human-robot interaction and virtual reality. This problem used to be hard to solve, because some traditional radio-based localization methods such as GNSS, WiFi, UWB, suffer from serious attenuation, multipath effect and distortion in indoor areas, especially in the presence of moving people and a great amount of obstacles and concrete reinforcement walls. However, the appearance of magneto-inductive device (MI) using low-frequency, quasi-static magnetic fields, provides another possibility to handle localization problem in challenging areas by being less influenced by those distortion factors. Moreover, the widespread implementation and increasing accuracy of small-size MEMS inertial sensors (IMU) expects a promising future to give odometry without the need for external references in a period of time. In this paper, we exploit the sensor information from IMU and MI to achieve long-term large-scale indoor localization by making following contributions: we presented a highly-coupled integration method between IMU and MI sensors, which could mitigate high system error drifts of IMU, and low data-rate problem of MI; a novel Kalman filter framework, named Range-Constrained Kalman Filter (RCKF) was proposed to combine strapdown inertial navigation system (SINS) with motion characteristics and range measurement; a robust indoor localization system architecture was designed and tested in real experiments. On low-cost IMU and MI platform, the results from our proposed integration method show a significant improvement than that without range constraints. 90-percentile error of our localization systems is within 5-6 meter in our experiment with a total walking distance of 730 meter.

I. INTRODUCTION

Over the past decade, the advances of MEMS (Micro-electro-mechanical Systems) technology enable the wide spread of various sensors in our normal lives, such as accelerometer, gyroscope, magnetometer, barometer, which can help sense environmental or movement alterations, and constitute huge perception mobile networks of sensors. Users positions in indoor area are crucial information in location-based services, human-robot interaction and virtual reality (VR). How to exploit the information provided by sensors around us and realize reliable indoor localization has received great attention from both academics and industries [1] [2] [3].

For indoor pedestrian localization, some of common localization methods might be inappropriate in these challenging

areas. For example, GNSS signal are probably blocked, attenuated or suffer from multi-path effect, and hence hardly satisfy user's requirements for indoor localization [4]. Moreover, visual-inertial odometry or visual SLAM, which is widely applied in robot navigation, might be not practical for pedestrian because of its great computational demand, high energy consumption and high requirement of environment light. Compared with radio or visual localization, strapdown inertial navigation system (SINS) has little dependence on environmental effects, is quite light-weight and can run real time on mobile chips. It's a process of integrating angular rate into attitudes, transforming measured acceleration into navigation coordinate frame, integrating navigation frame velocity into position, where acceleration and angular velocity are easy to provided by accelerometers and gyroscopes under low energy consumption [5] [6].

For normal users, the size and cost of MIMU (MEMS Inertial Measurement Unit) implemented are extremely limited, leading to high noises of accelerometers and gyroscopes, and system drifts of SINS are increasing exponentially with the passage of time[7]. Therefore, constraints from behavioral or environmental contexts have to be imposed to SINS in order to reduce error drifts and improve robustness of navigation system[8]. For behavioral context, MIMU attached to shoes, wrist, in hand or in pocket have different motion characteristics[9]. For example, according to periodic characteristics of human walking, Zero-velocity update (ZUPT) or Zero-Angular update could be used to compensate system error, when detecting pedestrian are in still phase[10]. For environmental context, information from other sources, such as magnetic field, gravity field, optical flow, could be combined together with inertial system in order to improving robustness of navigation system [11] [12] [13].

State estimation and information fusion algorithm combining behavioral context or other sensors with inertial sensors determine a good design of an accurate, reliable and robust localization system. A typical way is Kalman Filter, which has been widely, successfully applied in guidance, navigation, and control of vehicles, aircraft, spacecraft and robotics after its appearance for over 50 years, due to its high efficiency, robustness and low computation requirement [14]. In the field of indoor localization, Kalman filter also has a great amount of good applications in states estimation from different sensor sources [15] [16] [17]. In order to improve the property of Kalman filtering, we propose a novel range-constrained Kalman filter (RCKF), a highly-coupled integration of inertial sensors with range measurement sensors, which can enhance properties of a standard Kalman

This work was a reading course report of Department of Computer Science, University of Oxford.

The Authors are with Department of Computer Science, University of Oxford, 15 Parks Rd, Oxford, United Kingdom, OX1 3QD, (changhao.chen@cs.ox.ac.uk; andrew.markham@cs.ox.ac.uk; niki.trigoni@cs.ox.ac.uk)

Filter, if range information is available. A good thing is that the implementation of this kind of improved Kalman Filter does not require any change of the navigation system states and transition models, that have already been built for a standard Kalman filter, and leaves prediction process and update process unchanged.

Some radio-based technologies could provide range measurements in indoor areas, by using received signal strength indication (RSSI) or the Time of Flight (ToF) between transmitters and receivers, for example, RFID, UWB and Wifi [18]. Compared with cameras or lasers, they could operate when there is no direct Line of Sight (LOS) and in long distance. However, due to the use of high frequencies, their signals are easily delayed, attenuated or suffer from multi-path, when propagating through complex lossy bodies, or in non-line-of-sight (NLoS) environments [19]. These drawbacks limit their further use in challenging areas, especially in indoor localization. In our approach, a reliable range estimation (distance between transmitter and receiver) is extremely crucial when applied into Kalman filter with range constraints mentioned above. Here, we integrated a magneto-inductive (MI) device based on low-frequency, quasi-static magnetic fields into our system instead of propagating radio waves. An important advantage of MI is that obstacles such as walls, floors, and people that heavily influence the property of high frequency radio, are largely transparent to the quasi-static magnetic fields [20]. The low-data-rate problem of MI could be mitigated by integrating with imu which could measure up to 200 Hz in a normal mobile device.

The main contributions of this paper are summarized as follows:

- 1) We presented a highly-coupled integration method between IMU and MI sensors, which could mitigate high system error drifts of IMU and low data rate problem of MI;
- 2) A novel Kalman filter framework, named Range-Constrained Kalman Filter (RCKF) was proposed to combine strapdown inertial navigation system (SINS) with motion characteristics and range measurement;
- 3) A robust indoor localization system was designed and tested in real experiments.

The rest of this paper is structured as follows. Section 2 reviews related work. Our system overview and the design of a standard Kalman Filter based on motion characteristics are illustrated in Section 3 and 4, respectively. In Section 5, an improved Kalman filter, named Range-Constrained Kalman Filter (RCKF), is derived according to mathematical model of distance constraints and Bayesian estimation. Section 6 presents how to estimate distances between receiver and transmitter from RSSI of MI signals, and locations of MI transmitters based on path-loss propagating model. In Section 7 and 8, the experimental results are illustrated to support the validity of our proposal method and show the accuracy of localization system, and then the conclusions and future work are summarized.

II. RELATED WORK

A great amount of research work has been conducted on the problem of indoor localization. With the spread of indoor wireless devices (WiFi, Bluetooth), the combination of IMU and RSSI attracted attentions from academics to acquire hybrid localization results. Most of them are realized through WiFi or UWB, which suffer from lots of troubles in NLoS environments. Our approach is related with the combination of IMU and RSSI, Kalman filter with state constraints, and magneto-inductive technologies, whose developments will be discussed respectively in this section.

A. Integration of IMU and RSSI

Some researchers combined inertial navigation system with RSSI from WiFi or UWB signals. For example, [21] used WiFi RSSI to initiate starting location, and determined a only gross region space, where user was located in, for a foot-mounted inertial pedestrian system. In [22]’s work, Particle Filter (PF) was applied into fusion of WiFi and PDR. Although PF didn’t require linearization for range constraints, it suffered from great computational load and was probably stuck in local minimum, bringing troubles to mobile platform. Researcher [23] presented a study of improvements resulting from inclusion IMU into an RSSI localization wireless sensor networks (WSN) using Kalman filter. It simply incorporated positions estimation from PDR into WSN in a loosely-coupled way, and therefore the accuracy of a fusion system didn’t show a significant improvement compared with RSS only WSN. In Range-Only SLAM problem, odometry (mainly visual odometry in robotics) and range from radio signals were combined together into KF-based SLAM, and could estimate localizations of robotics and transmitters at the same time[18]. However, our work mainly focused on integration of inertial odometry and range from MI, and mapping problem was out of our concern. To be noticeable, [24] reported a first trivial to design a tightly-coupled integration for WiFi and IMU by linearizing range constraints, and placing they into system model and observation model of Kalman Filter. However, KF is only linear projection operator and this nonlinear constraints are fundamentally different from linear constraints, which will cause troubles in some situations. Moreover, this method required to increase the dimension of system states of Kalman filter, and computation may be a problem with the increase of number of transmitters. In compared, the tightly-coupled approach we proposed doesn’t suffer from these problems.

B. Kalman Filter with state constraints

Although Kalman Filter and its modifications (unscented Kalman Filter, extended Kalman Filter) are powerful tools for state estimation, some information about a system might not be easily incorporated in, for example, the system states satisfy equality constraints (e.g. range constraints in our localization system). Therefore, some researchers modified Kalman filter to exploit additional information and improved its performance[14]. [25] proposed a method to project unconstrained Kalman filter onto the state constraint surface,

but it only considered linear equality and might not be appropriate for our range-constrained problem. In order to solve nonlinear state constraints problem, [26] presented a new method that utilized the projection method twice, while [27]’s approach considered a second-order approximation to an arbitrary nonlinearity of state constraints. All of their work only have simulation results. Our approach based on some work from [25] [27], further derived an Kalman Filter with range constraints (range-constrained KF, RCKF) using Bayesian estimation, which fits our problem well.

C. Magneto-Inductive Technologies

Magnetic field has long been used for navigation, since magnetic compass was applied in nautical navigation in ancient times. Nowadays, magnetometers have already been cheap and small enough to be implemented in mobile phones. Geomagnetic heading was considered as reference vector for indoor pedestrian navigation, but an abundance of metal in indoor environment, such as in steel-reinforced buildings, can vary magnetic heading greatly from real values[28]. An attempt to set geomagnetic distortion as landmarks in graph-SLAM proved to be valid in rich magnetic interference places, but still troubled with detecting loop closure, since magnetic distortion features are not easy to distinguish with each other[29]. These years, a promising solution generating extremely low-frequency, quasi-static magnetic field appeared, and proved to be an excellent technology to measure distances between transmitters and receivers [30] [31] [32] [20] [33] in challenging areas. Unlike traditional high-frequency radio-based methods (WiFi, UWB, RFID), the low-frequency magnetic field experience no multi-path effect or shadow fading in non-line-of-sight (NLoS) environments. These attractive properties make it a good replacement for indoor localization, where people are continuously moving, and walls, floors and obstacles may impact high frequency radio. Therefore, magneto-inductive (MI) devices are selected in our localization system as range measurement method, which will definitely mitigate the troubles that high-frequency radio-based approaches bring [18] [24], and enable long-term large-scale localization.

III. SYSTEM OVERVIEW

In this section, we provide an overview of main components in our localization system, illustrated in figure 1.

IMU (Inertial Measurement Units) senses user’s movement with acceleration and angular velocity rate measurements, which are through navigation equations of SINS transformed into pose attitudes, velocities and positions. In order to constrain error drifts of inertial system, Kalman filter based on error models of SINS is designed to exploit user’s motion characteristics or context information.

MI (Magneto-Inductive Device) is composed of triaxial transmitters generating low-frequency quasi-static magnetic field, and receivers with triaxial receiving coils, which detect the low-frequency magnetic field. The channel matrix from receiver could be converted into signal RSSI or used to detect whether signal is distorted. Transmitters’ locations could be

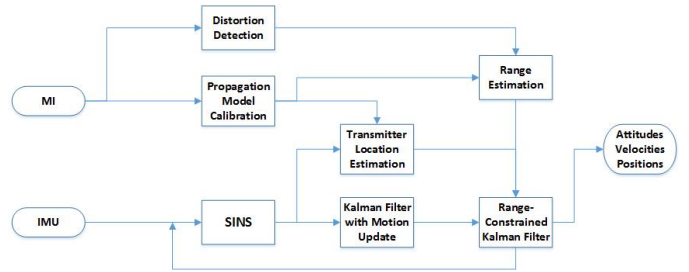


Fig. 1: system overview

obtained with the help of inertial odometry provided by IMU. Range (distance between user and transmitters) is estimated through path-loss model from a calibrated propagation model.

The highly-coupled integration approach we proposed in this paper combine inertial navigation system with the range measurement provided by MI. The system states from range-constrained Kalman filter are feed back to SINS to correct system error drifts, and output navigation information at every time step for users.

IV. STANDARD KALMAN FILTER DESIGN

Low-cost IMU implemented in our system suffers seriously from high measurement noises, which causes exponentially accumulating errors of inertial navigation system. Therefore, a real-time dynamic process of error drifts compensation is a necessity for maintaining long-term navigation. For indoor pedestrian navigation, motion characteristics of human walking provide useful background information, while error model based Kalman filter can take full advantages of motion characteristics and satisfy requirements of real-time dynamic state estimation. In this section, we introduced a design of unconstrained Kalman Filter (unconstrained refers to without range constraints) using motion characteristics and error models of SINS System, to predict and compensate the error drifts of real-time inertial navigation system.

A. Transition Model Design based on Error Model

Our SINS-based pedestrian navigation system is designed as 15 states \mathbf{x} at any given time step: pose attitudes $\phi \in \mathbb{R}^3$, velocities $\mathbf{v} \in \mathbb{R}^3$, positions $\mathbf{r} \in \mathbb{R}^3$, gyroscope biases $\mathbf{b}_g \in \mathbb{R}^3$, and acceleration biases $\mathbf{b}_a \in \mathbb{R}^3$.

$$\mathbf{x} = [\phi \quad \mathbf{v} \quad \mathbf{r} \quad \mathbf{b}_g \quad \mathbf{b}_a]^T \quad (1)$$

At every time step k , we use measurements, namely acceleration $a_k \in \mathbb{R}^3$ from accelerometer and angular rate $\omega_k \in \mathbb{R}^3$ from gyroscope to update navigation system states.

$$\mathbf{x}_k = f(\mathbf{x}_{k-1}, \mathbf{a}_k, \omega_k) + \delta \mathbf{x}; \quad (2)$$

$\delta \mathbf{x}$, representing error states of navigation system states, is crucial in maintaining long-term navigation, by being estimated dynamically through Kalman Filter, and deliver error estimates back to INS. Error state δx is defined as follows:

$$\delta \mathbf{x} = [\delta \phi \quad \delta \mathbf{v} \quad \delta \mathbf{r} \quad \mathbf{b}_g \quad \mathbf{b}_a]^T \quad (3)$$

Its transition equation and observation equation are approximated following linear system states transition.

$$\delta \dot{\mathbf{x}} = \mathbf{F} \delta \mathbf{x} + \mathbf{G} \mathbf{u} + \mathbf{w} \quad (4)$$

$$\mathbf{z} = \mathbf{H} \delta \mathbf{x} + \boldsymbol{\nu} \quad (5)$$

where, \mathbf{F} represents state transition model, \mathbf{G} represents control-input model with respect to control vector \mathbf{u} , \mathbf{z} is observation states, and \mathbf{H} is observation model mapping the error states to observed space, while \mathbf{w} , $\boldsymbol{\nu}$ are process noises and observation noises, respectively, which are assumed to be Gaussian white noises. A discussion about transition model and observation model will be given later.

The state transition matrix of Kalman filter \mathbf{F} is built on error modeling of inertial navigation system[34]. Although our localization system adopts low-IMU, we found that the influence of earth rotation still should not be ignored, especially when the accuracy of MEMS IMU implemented in mobile devices is increasing gradually.

$$\mathbf{F} = \begin{bmatrix} \mathbf{F}_{11} & \mathbf{0} & \mathbf{0} & \mathbf{0} & \mathbf{C}_b^n \\ \mathbf{F}_{21} & \mathbf{F}_{22} & \mathbf{0} & \mathbf{C}_b^n & \mathbf{0} \\ \mathbf{0} & \mathbf{I} & \mathbf{0} & \mathbf{0} & \mathbf{0} \\ \mathbf{0} & \mathbf{0} & \mathbf{0} & \mathbf{0} & \mathbf{0} \\ \mathbf{0} & \mathbf{0} & \mathbf{0} & \mathbf{0} & \mathbf{0} \end{bmatrix} \quad (6)$$

$$\mathbf{G} = \begin{bmatrix} -\mathbf{C}_b^n & \mathbf{0} & \mathbf{0} & \mathbf{0} \\ \mathbf{0} & \mathbf{C}_b^n & \mathbf{0} & \mathbf{0} \\ \mathbf{0} & \mathbf{0} & \mathbf{0} & \mathbf{0} \\ \mathbf{0} & \mathbf{0} & \mathbf{I} & \mathbf{0} \\ \mathbf{0} & \mathbf{0} & \mathbf{0} & \mathbf{I} \end{bmatrix} \quad (7)$$

where, the rotation matrix \mathbf{C}_b^n transforms vectors from body-frame ordinates to local navigation frame ordinates (North-East-Down). Matrix \mathbf{F}_{11} and \mathbf{F}_{22} are related with Earth's rotation speed Ω and user's latitude L . Matrix \mathbf{F}_{21} is with respect with the skew-symmetric cross-product operator matrix of accelerometer measurements $\mathbf{f}^n = [f_N \quad f_E \quad f_D]^T$ in navigation frame .

$$\mathbf{F}_{11} = \begin{bmatrix} 0 & -\Omega \sin L & 0 \\ \Omega \sin L & 0 & \Omega \cos L \\ 0 & -\Omega \cos L & 0 \end{bmatrix} \quad (8)$$

$$\mathbf{F}_{21} = \begin{bmatrix} 0 & -f_D & f_E \\ f_D & 0 & -f_N \\ -f_E & f_N & 0 \end{bmatrix} \quad (9)$$

$$\mathbf{F}_{22} = \begin{bmatrix} 0 & -2\Omega \sin L & 0 \\ 2\Omega \sin L & 0 & 2\Omega \cos L \\ 0 & -2\Omega \cos L & 0 \end{bmatrix} \quad (10)$$

B. Observation Model Design based on Context Constraints

In measurement equation, the observation model \mathbf{H} is determined by the states which can be observed in our navigation systems. For example, in Zero-Velocity Update (ZUPT), a foot-mounted IMU could sense user's motion, and divide user's status into swinging and still phases by gait analysis algorithms. In this situation, velocities are observable, and assumed to be zero, when detecting still phases, which appear periodically in pedestrian walking[17]. The observation model \mathbf{H} is designed as

$$\mathbf{H} = [\mathbf{0}_{3 \times 3} \quad \mathbf{I}_{3 \times 3} \quad \mathbf{0}_{3 \times 3} \quad \mathbf{0}_{3 \times 3} \quad \mathbf{0}_{3 \times 3}] \quad (11)$$

In Zero-Angular Update (ZARU), the angular rates of rigid body (e.g. feet or leg) attached by IMU are assumed to be zero in still phases, and hence its errors $\delta \boldsymbol{\omega} = [0 \quad 0 \quad 0] - \boldsymbol{\omega}$ are observable[35]. Therefore, \mathbf{H} is designed as follows.

$$\mathbf{H} = [\mathbf{0}_{3 \times 3} \quad \mathbf{0}_{3 \times 3} \quad \mathbf{0}_{3 \times 3} \quad \mathbf{I}_{3 \times 3} \quad \mathbf{0}_{3 \times 3}] \quad (12)$$

When environment information is available, for example, receiving heading attitude from geomagnetic field [15] [36] or solving perspective-n-point problem of computer vision[16] [37], or acquiring pitch and roll attitudes from gravity field[11], the errors states of users' pose attitudes could be obtained in our system. Therefore, \mathbf{H} is designed as follows.

$$\mathbf{H} = [\mathbf{I}_{3 \times 3} \quad \mathbf{0}_{3 \times 3} \quad \mathbf{0}_{3 \times 3} \quad \mathbf{0}_{3 \times 3} \quad \mathbf{0}_{3 \times 3}] \quad (13)$$

If the motion constraints and environment constraints mentioned above are available at the same time, a observation model \mathbf{H} could combine all of them together to improve system's robustness.

$$\mathbf{H} = \begin{bmatrix} \mathbf{I}_{3 \times 3} & \mathbf{0}_{3 \times 3} & \mathbf{0}_{3 \times 3} & \mathbf{0}_{3 \times 3} & \mathbf{0}_{3 \times 3} \\ \mathbf{0}_{3 \times 3} & \mathbf{I}_{3 \times 3} & \mathbf{0}_{3 \times 3} & \mathbf{0}_{3 \times 3} & \mathbf{0}_{3 \times 3} \\ \mathbf{0}_{3 \times 3} & \mathbf{0}_{3 \times 3} & \mathbf{0}_{3 \times 3} & \mathbf{I}_{3 \times 3} & \mathbf{0}_{3 \times 3} \end{bmatrix} \quad (14)$$

Through predict and update processes of Kalman filter as follows, an optimal estimation of error states $\delta \mathbf{x}_k$ are recursively computed and feed back to SINS to compensate system drifts.

$$\mathbf{K}_k = \mathbf{P}_{k|k-1} \mathbf{H}_k^T (\mathbf{H}_k \mathbf{P}_{k|k-1} \mathbf{H}_k^T + \mathbf{R}_k)^{-1} \quad (15)$$

$$\delta \mathbf{x}_k = \delta \mathbf{x}_{k|k-1} + \mathbf{K}_k (\mathbf{Z}_k - \mathbf{H}_k \delta \mathbf{x}_{k|k-1}) \quad (16)$$

$$\mathbf{P}_k = (\mathbf{I} - \mathbf{K}_k \mathbf{H}_k) \mathbf{P}_{k|k-1} (\mathbf{I} - \mathbf{K}_k \mathbf{H}_k)^T + \mathbf{K}_k \mathbf{R}_k \mathbf{K}_k^T \quad (17)$$

$$\mathbf{P}_k = (\mathbf{I} - \mathbf{K}_k \mathbf{H}_k) \mathbf{P}_{k|k-1} \quad (18)$$

Finally, a drifts-reduced navigation system state $\hat{\mathbf{x}}_k$ is updated with our estimation of error states using unconstrained Kalman Filter.

$$\hat{\mathbf{x}}_k = \mathbf{x}_k + \delta \mathbf{x}_k \quad (19)$$

V. RANGE-CONSTRAINED KALMAN FILTER

Although system drifts are reduced through context constraints by Kalman filter to a certain extent, the accuracy of observation measurements and linearisation of error model still determine properties of Kalman filter, as well as the accuracy of navigation system. For example, in ZUPT, the biases of still phase detection will deteriorate the estimation of error states, and impact updated system states. Additional information, referring to range constraints in our problem, could improve accuracy of error states estimation and reduce their covariance. This section introduced derivation of a novel Kalman Filter frame, range-constrained Kalman filter (RCKF) based on some work of Kalman filter with equality constraints from [25][27]. Our proposed method will be tested in real experiments in next section.

Compared with the estimation of unconstrained KF \hat{x} , we define optimal estimation of constrained KF as \check{x} . Consider a scenario where navigation states obey a nonlinear range equality, which is the distance between user's location states and transmitter equal to distance measurement provided through RSSI. That is

$$\|\mathbf{D}\mathbf{x} - \mathbf{r}_e\|_2 = d \quad (20)$$

where, the matrix $\mathbf{D} = [\mathbf{0}_{3 \times 3} \quad \mathbf{0}_{3 \times 3} \quad \mathbf{I}_{3 \times 3} \quad \mathbf{0}_{3 \times 3} \quad \mathbf{0}_{3 \times 3}]$ maps entire navigation states to only location states, \mathbf{r}_e is location of MI transmitter inferred from RSSI log-distance path loss model, and d is distance between pedestrian and MI transmitter.

One solution to find the optimal estimate of constrained system states is to derive constrained Kalman Filter by using maximum probability. Kalman filter estimate can be viewed as searching an estimate of state \mathbf{x} by maximizing the conditional probability density function given observation \mathbf{z} .

$$pdf(\mathbf{x}|\mathbf{z}) = \frac{\exp(-(\mathbf{x} - \bar{\mathbf{x}})^T \boldsymbol{\Sigma}^{-1}(\mathbf{x} - \bar{\mathbf{x}})/2)}{(2\pi)^{n/2} |\boldsymbol{\Sigma}|^{1/2}} \quad (21)$$

where, $\boldsymbol{\Sigma}$ is the covariance of the Kalman Filter estimate, and $\bar{\mathbf{x}}$ represents the conditional mean of \mathbf{x} .

The constrained Kalman filter can be derived by finding an estimate $\check{\mathbf{x}}$ under the condition that its conditional probability $pdf(\check{\mathbf{x}}|\mathbf{z})$ is maximized and $\check{\mathbf{x}}$ satisfies the constraints 20 [25]. So our problem is converted into

$$\begin{cases} \check{\mathbf{x}} = \arg \max_{\mathbf{x}} pdf(\mathbf{x}|\mathbf{z}) \\ \|\mathbf{D}\mathbf{x} - \mathbf{r}_e\|_2 = d \end{cases} \quad (22)$$

To be noticeable, since $\arg \max_{\mathbf{x}} pdf(\mathbf{x}|\mathbf{z})$ equals to $\arg \min_{\mathbf{x}} (\mathbf{x} - \bar{\mathbf{x}})^T \boldsymbol{\Sigma}^{-1}(\mathbf{x} - \bar{\mathbf{x}})$, equation 22 can be regarded as finding minimum value under constraints, and therefore we form Lagrangian equation to solve our problem:

$$L(\mathbf{x}, \lambda) = f(\mathbf{x}) + \lambda \psi(\mathbf{x}) \quad (23)$$

$$\begin{cases} f(\mathbf{x}) = (\mathbf{x} - \bar{\mathbf{x}})^T \boldsymbol{\Sigma}^{-1}(\mathbf{x} - \bar{\mathbf{x}}) \\ \psi(\mathbf{x}) = \|\mathbf{D}\mathbf{x} - \mathbf{r}_e\|_2^2 - d^2 \end{cases} \quad (24)$$

The stationary point of the Lagrangian function 23 is given by solving first partial derivative.

$$\frac{\partial f(L)}{\partial \mathbf{x}} = 0 \implies \frac{\partial f(\mathbf{x})}{\partial \mathbf{x}} + \frac{\partial \lambda \psi(\mathbf{x})}{\partial \mathbf{x}} = 0 \quad (25)$$

$$\frac{\partial L}{\partial \lambda} = 0 \implies \psi(\mathbf{x}) = 0 \quad (26)$$

This is given by

$$\frac{\partial f(L)}{\partial \mathbf{x}} = 2(\mathbf{x} - \bar{\mathbf{x}})^T \boldsymbol{\Sigma}^{-1} + \lambda(2\mathbf{x}^T \mathbf{D}^T \mathbf{D} - \mathbf{D} \mathbf{r}_e - \mathbf{r}_e^T \mathbf{D}) = 0 \quad (27)$$

$$\psi(\mathbf{x}) = \mathbf{x}^T \mathbf{D}^T \mathbf{D} \mathbf{x} - \mathbf{x}^T \mathbf{D} \mathbf{r}_e - \mathbf{r}_e^T \mathbf{D} \mathbf{x} + \mathbf{r}_e^T \mathbf{r}_e - d^2 \quad (28)$$

The conditional mean $\hat{\mathbf{x}}$ refers to the estimate of standard Kalman filter, so the constrained estimate $\check{\mathbf{x}}$ could be obtained from unstrained estimate from equation 27 as follows.

$$\check{\mathbf{x}} = (\boldsymbol{\Sigma}^{-1} + \lambda \mathbf{D}^T \mathbf{D})^{-1} (\boldsymbol{\Sigma}^{-1} \hat{\mathbf{x}} + \frac{1}{2} \lambda (\mathbf{r}_e^T \mathbf{D} + \mathbf{D}^T \mathbf{r}_e)) \quad (29)$$

Further λ is derived by placing constrained estimate $\check{\mathbf{x}}$ into equation 28:

$$\lambda = \{\lambda \in \mathbb{R}^+ \mid \psi(\check{\mathbf{x}}, \lambda) = 0\} \quad (30)$$

Solving polynomial function 30 is to find its roots by adopting some roots-finding methods such as Newton's method [25]. Therefore, an estimate of range-constrained Kalman filter is derived.

When multiple distance constraints are available meanwhile, the k-th constrained estimate could be conducted from (k-1)-th constrained estimate, by viewing (k-1)-th constrained estimate as "unconstrained" estimate (an estimate without k-th constraint):

$$\begin{cases} \check{\mathbf{x}}_k = (\boldsymbol{\Sigma}^{-1} + \lambda \mathbf{D}^T \mathbf{D})^{-1} (\boldsymbol{\Sigma}^{-1} \check{\mathbf{x}}_{k-1} + \frac{1}{2} \lambda (\mathbf{r}_e^T \mathbf{D} + \mathbf{D}^T \mathbf{r}_e)) \\ \lambda = \{\lambda \in \mathbb{R}^+ \mid \psi(\check{\mathbf{x}}_k, \lambda) = 0\} \end{cases} \quad (31)$$

For our approach mentioned above, the unconstrained estimate is projected onto the surface of constrained space, and suffer less linearization troubles compared with placing range constraints directly into KF states [24]. Another advantage is that the prediction and update processes of Kalman filter could stay unchanged. Besides, there are no changes in system models and observation models built for a standard KF, which means the dimension of problems doesn't have to be increased. Compared with standard KF-based integration method, our approach saves memory and computation, especially when the number of range observations increases with the number of transmitters.

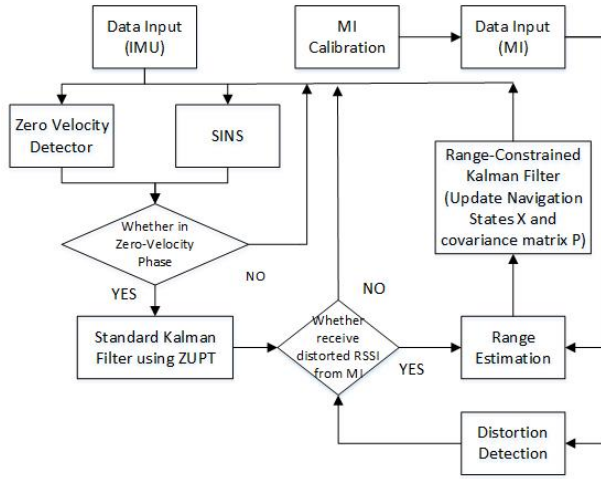


Fig. 2: Flow Map of Pedestrian Navigation based on ZUPT and range constraints.

VI. RANGE ESTIMATION FROM RSSI

An accurate estimation of distance between user and transmitters determines the property of RCKF mentioned in last section. In this section, we introduced a method of inferring locations of MI transmitters and RSSI range using log-distance path loss model.

The channel matrix \mathbf{S} in MI device represents the energy transferring from transmitter coils to receiver coils from a energy perspective[20]. We define the Frobenius norm of channel matrix $\|\mathbf{S}\|_F$ as the amount of received power, which is in free-space is proportional to the inverse cube of the range. Therefore, the overall RSSI of magneto-inductive device is measured in dB as

$$\rho \triangleq 20 \log_{10} \|\mathbf{S}\|_F \quad (32)$$

However, the existence of abundant metal in indoor environment impacts the RSSI model of Magneto-inductive device selected in our localization system. Thus, a calibration of propagation model is necessary by using log-distance path loss model. In this process, the locations of MI could be estimated at the same time.

$$\rho = \rho_0 + 10 n \log_{10}(d) \quad (33)$$

$$d = \|\mathbf{r}_{user} - \mathbf{r}_{MI}\|_2 \quad (34)$$

where, ρ_0 is the path loss at a reference distance of 1 meter, n is path loss exponent and d is the distance between user and MI transmitter, which is Euclidean metric from user's locations \mathbf{r}_{user} and transmitters' locations \mathbf{r}_{MI} .

Moreover, in the presence of large amounts of metal in indoor area, energy transferring relation between transmitter coils and receiver coils differs from that in undistorted area. Hence, with the help of channel matrix $\|\mathbf{S}\|_F$, we may detect the distorted range before applying in Range-Constrained KF, reducing the possibilities of wrong constraints. To get rid

of influences of receiver orientation, a orientation invariant matrix \mathbf{C} is defined

$$\mathbf{C} \triangleq \mathbf{S}^T \mathbf{S} \quad (35)$$

The coupling relation between transmitter coils and receiver coils could be reflected in how the eigenvalues of \mathbf{C} are spread. Therefore, we define the departure of the estimated eigenvalues $\hat{\lambda}$ from the eigenvalues in free-space areas λ [20]:

$$\mathfrak{S}(\hat{\lambda}) = \frac{\|\hat{\lambda} - \lambda\|_2}{\|\lambda\|_2} \quad (36)$$

If $\mathfrak{S}(\hat{\lambda})$ exceeds a threshold α , the estimated range from MI RSSI is considered to be distorted, and then discarded.

In short period of time, inertial navigation system using motion-characteristics-based Kalman filter provide reliable locations for user. Therefore, propagation model and transmitter locations could be estimated through the locations provided by IMU.

An algorithm flow map of pedestrian navigation system using ZUPT and range constraints is illustrated in the Figure 2.

VII. EXPERIMENTS

In this section, we will test the integration method we proposed in section 5, and our navigation system in real experiments. The results will be compared with the method without range constraints.

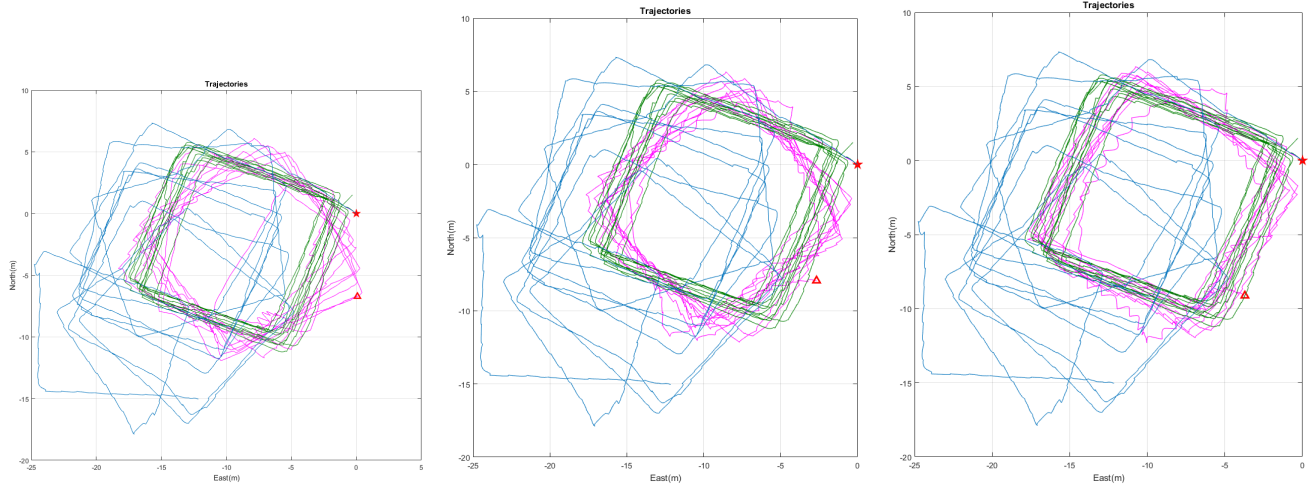
A. Experiment with ideal distance measurements

In order to evaluate the validity and efficiency of the method we proposed, we designed an experiment assuming that measured distances between users and transmitters are true values and received at every time epoch idealistically.

In this experiment, a extremely low-cost Imu MPU6050 (cost below 10 pounds) was selected as our experiment platform, which was attached to user's shoe. In ideal conditions, range update applied in our RCKF is assumed as true values, by calculating from distance between true positions (ground truth) and a fixed point selected in map. Our system was tested in an office building. We walked around a square (12m*12m) for 10 circles with a trajectory of half kilometer.

Due to the high sensor noises of MPU6050, the trajectories generated from SINS and KF without range constraints (shown as blue lines in Figures 3a-3c) will gradually deviate from ground truth (shown as green lines in Figures 3a-3c). Three fixed points (-5,-10), (-2,-10), (-12,-8) in the map are selected and assumed as transmitter locations. At every step, we update the range measurement by calculating the distance between locations from ground truth and fixed point, and place them into our integration algorithm RCKF proposed in Section 5. The number of "transmitters" which means the number of range constraints are changed from one to three and applied in our system respectively.

The results from RCKF are illustrated as trajectories (Purple Lines) in Figures 3a-3c), which are all closer to



(a) SINS and RCKF with one constraint (b) SINS and RCKF with two constraints (c) SINS and RCKF with three constraints
 Fig. 3: Trajectories from SINS and RCKF with one constraint (a), two constraints (b), and three constraints (c)

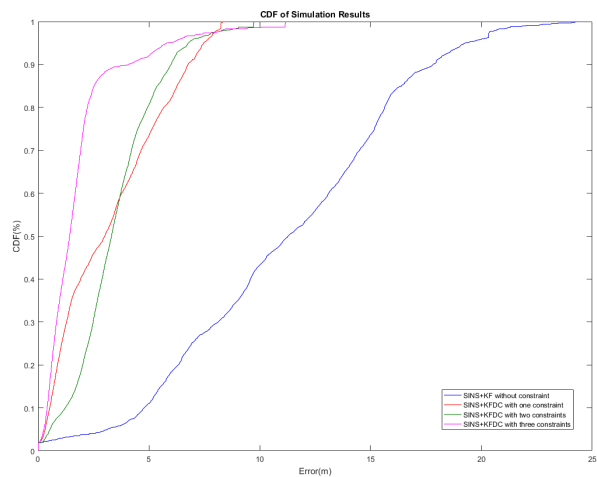


Fig. 4: CDF of positioning errors in Experiment 1

the true positions (Green Lines) compared with the results without range constraints (Blue Lines). Figure 4 shows that in 90% test time, position errors of our localization systems are below 6.8 meter, 6 meter and 3.6 meter when our system has ideal range constraints with one to three transmitters respectively, shows a great improvement compared with previous position error of 18 meter in system without range constraints.

B. Experiment with Magneto-Inductive Range Measurement

The goal of this experiment is to evaluate the accuracy of our proposed localization system with range measurements from real magneto-inductive RSSI. Compared with WiFi, MI shows an excellent stability in presence of moving people, and its range accuracy and sensibility is much more reliable in large-scale indoor areas in the condition that user pass through multiple floors and rooms[20].

This experiment was conducted on the third floor and fourth floor of an office building. Three MI transmitters

(TR1, TR2, TR3) were placed in three fixed points, whose locations would be estimated through the method proposed in section 6. User with MI receiver and IMU walked in a trajectory of more than 730 meter. The ground truth of trajectory was obtained by using Tango, shown as the green lines of figures 5a-5c.

The localizations of MI transmitters were estimated through inertial odometry provided by IMU, drawn as black boxes in figures 5a-5c. The range measurements between user and transmitters were estimated through propagation model of MI and distortion detection criterion, and finally feed into range-constrained Kalman filter. The results of RCKF were illustrated as generated trajectories (red lines), and compared with results from unconstrained Kalman filter (blue lines) in figures 5a-5c. Figure 6 shows the cumulative distribution function of error functions from unconstrained KF (blue line), range-constrained KF using TR1 (green line), TR2 (red line) and TR3 (purple line) respectively. In 90 % time, our experiment could reach a position errors below 5-6 meter in a total distance of 730 meter.

VIII. CONCLUSIONS

Locations are key information in multiple applications such as location-based services, warehousing, human-robot interaction, and virtual reality. Accurate reliable indoor positioning used to be hard to solve, because some traditional radio-based localization methods such as GPS, WiFi, UWB, suffer from serious attenuation, multi-path effect and distortion in indoor areas, especially in the presence of moving people and a great amount of obstacles and concrete reinforcement walls. However, the appearance of magneto-inductive device (MI) which generates low-frequency, quasi-static magnetic fields, provides another possibility to handle localization problem in challenging areas. Compared with GPS, WiFi and UWB, MI is less influenced by these indoor factors. In this paper, we exploit the inertial information provided by low-cost MEMS IMU to design strapdown

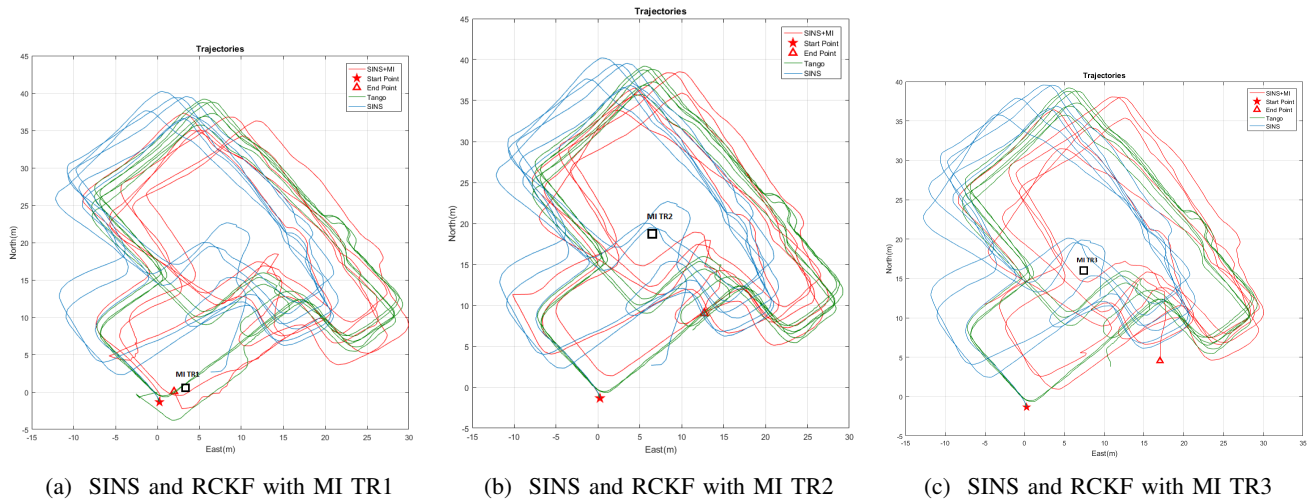


Fig. 5: Trajectories from SINS and RCKF with MI TR1 (a), MI TR2 (b), and MI TR3 (c)

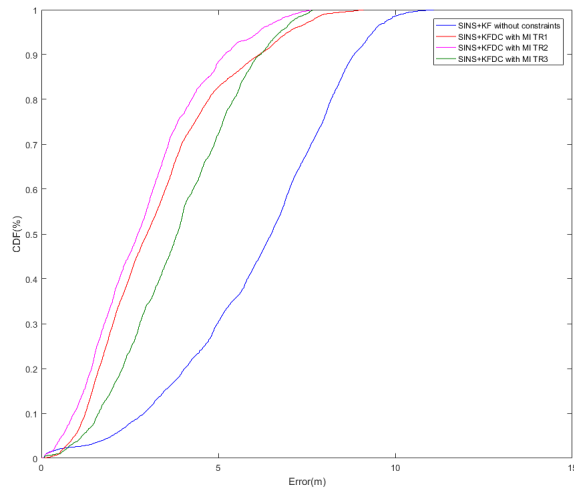


Fig. 6: CDF of positioning errors in Experiment 2

inertial navigation system, and apply motion characteristics to reduce system error drifts. In order to achieve long-term large-scale localization, magneto-inductive range measurements are tightly-coupled integrated into inertial system to receive a more robust reliable odometry. We proposed a novel and quite light-weight fusion algorithm called range-constrained Kalman filter (RCKF) to solve this nonlinear equality constraint problem. Under several experiments, the results from the integration algorithm we proposed saw a great improvement compared with unconstrained results. We believe that a highly-couple integration of MI and IMU could overcome the high drifts problem of inertial sensors, and distorted and low data rate problem of MI, and will expect a promising future to provide more accurate reliable location information for users in indoor activities.

REFERENCES

[1] D. Lymberopoulos, J. Liu, X. Yang, R. R. Choudhury, V. Handziski, and S. Sen, "A Realistic Evaluation and Comparison of Indoor

Location Technologies: Experiences and Lessons Learned," *2015 International Conference on Information Processing in Sensor Networks, IPSN 2015*, no. Table 1, pp. 178–189, 2015.

- [2] Y. Shu, K. G. Shin, T. He, and J. Chen, "Last-Mile Navigation Using Smartphones," in *Proceedings of the 21st Annual International Conference on Mobile Computing and Networking, MobiCom*, pp. 512–524, 2015.
- [3] J. O. Nilsson, I. Skog, P. Händel, and K. V. S. Hari, "Foot-mounted INS for everybody - An open-source embedded implementation," *Record - IEEE PLANS, Position Location and Navigation Symposium*, pp. 140–145, 2012.
- [4] P. D. P. Groves, H. Martin, K. Voutsis, D. Walter, L. Wang, H. Marti, K. Voutsis, D. Walter, and L. Wang, "Context Detection, Categorization and Connectivity for Advanced Adaptive Integrated Navigation," *ION GNSS 2013*, no. September, pp. 1039 – 1056, 2013.
- [5] P. G. Savage, "Strapdown Inertial Navigation Integration Algorithm Design Part 1: Attitude Algorithms," *Journal of Guidance, Control, and Dynamics*, vol. 21, no. 1, pp. 19–28, 1998.
- [6] P. G. Savage, "Strapdown Inertial Navigation Integration Algorithm Design Part 2: Velocity and Position Algorithms," *Journal of Guidance, Control, and Dynamics*, vol. 21, no. 1, pp. 19–28, 1998.
- [7] I. Skog, J. O. Nilsson, P. Handel, and A. Nehorai, "Inertial Sensor Arrays, Maximum Likelihood, and Cramér-Rao Bound," *IEEE Transactions on Signal Processing*, vol. 64, no. 16, pp. 4218–4227, 2016.
- [8] P. D. Groves, L. Wang, D. Walter, H. Martin, K. Voutsis, and Z. Jiang, "The four key challenges of advanced multisensor navigation and positioning," in *IEEE PLANS, Position Location and Navigation Symposium*, no. May, pp. 773–792, 2014.
- [9] Z. Xiao, H. Wen, A. Markham, and N. Trigoni, "Robust pedestrian dead reckoning (R-PDR) for arbitrary mobile device placement," in *2014 International Conference on Indoor Positioning and Indoor Navigation, IPIN 2014*, no. October, 2014.
- [10] C. Chen, Z. Chen, X. Pan, and X. Hu, "Assessment of Zero-Velo city Detectors for Pedestrian Navigation System using MIMU," in *IEEE Chinese Guidance, Navigation and Control Conference*, pp. 128–132, 2016.
- [11] P. Zhou, M. Li, and G. Shen, "Use It Free: Instantly Knowing Your Phone Attitude," *Mobicom'14*, pp. 605–616, 2014.
- [12] M. H. Afzal, V. Renaudin, and G. Lachapelle, "Use of earth's magnetic field for mitigating gyroscope errors regardless of magnetic perturbation," *Sensors*, vol. 11, no. 12, pp. 11390–11414, 2011.
- [13] M. Li and A. I. Mourikis, "Vision-aided inertial navigation for resource-constrained systems," *IEEE International Conference on Intelligent Robots and Systems*, pp. 1057–1063, 2012.
- [14] D. Simon, "Kalman filtering with state constraints: a survey of linear and nonlinear algorithms," *IET Control Theory & Applications*, vol. 4, no. 8, p. 1303, 2010.
- [15] W. Li and J. Wang, "Effective Adaptive Kalman Filter for MEMS-IMU/Magnetometers Integrated Attitude and Heading Reference Systems," *Journal of Navigation*, vol. 66, no. 01, pp. 99–113, 2012.

- [16] C. Kessler, C. Ascher, N. Frietsch, M. Weinmann, and G. F. Trommer, "Vision-based attitude estimation for indoor navigation using vanishing points and lines," *Record - IEEE PLANS, Position Location and Navigation Symposium*, pp. 310–318, 2010.
- [17] I. Skog, P. Händel, J.-O. Nilsson, and J. Rantakokko, "Zero-velocity detection — an algorithm evaluation.," *IEEE transactions on bio-medical engineering*, vol. 57, no. 11, pp. 2657–2666, 2010.
- [18] F. R. Fabresse, F. Caballero, I. Maza, and A. Ollero, "Robust Range-Only SLAM for Unmanned Aerial Systems," *Journal of Intelligent and Robotic Systems*, pp. 1–14, 2015.
- [19] D. D. Arumugam, J. D. Griffin, D. D. Stancil, and D. S. Ricketts, "Measurements corner: Three-dimensional position and orientation measurements using magneto-quasistatic fields and complex image theory," *IEEE Antennas and Propagation Magazine*, vol. 56, no. 1, pp. 160–173, 2014.
- [20] T. E. Abrudan, Z. Xiao, A. Markham, and N. Trigoni, "Distortion Rejecting Magneto-Inductive Three-Dimensional Localization (MagLoc)," *IEEE JOURNAL ON SELECTED AREAS IN COMMUNICATIONS*, vol. 33, no. 11, pp. 1–14, 2015.
- [21] O. Woodman and R. Harle, "Pedestrian localisation for indoor environments," *2008 international conference on Ubiquitous computing-UbiComp 2008*, p. 114, 2008.
- [22] F. Evennou and F. Marx, "Advanced integration of WiFi and inertial navigation systems for indoor mobile positioning," *Eurasip Journal on Applied Signal Processing*, vol. 2006, pp. 1–11, 2006.
- [23] J. Schmid, T. Gadeke, W. Stork, and K. D. Muller-Glaser, "On the fusion of inertial data for signal strength localization," *Proceedings of the 8th Workshop on Positioning Navigation and Communication 2011, WPNC 2011*, pp. 7–12, 2011.
- [24] Y. Zhuang and N. El-Sheimy, "Tightly-Coupled Integration of WiFi and MEMS Sensors on Handheld Devices for Indoor Pedestrian Navigation," *IEEE Sensors Journal*, vol. 16, no. 1, pp. 224–234, 2016.
- [25] D. Simon and T. L. I. Chia, "Kalman filtering with state equality constraints," *IEEE Transactions on Aerospace and Electronic Systems*, vol. 38, no. 1, pp. 128–136, 2002.
- [26] S. J. Julier and J. J. LaViola, "On Kalman Filtering With Nonlinear Equality Constraints," *IEEE Transactions on Signal Processing*, vol. 55, no. 6, pp. 2774–2784, 2007.
- [27] C. Yang and E. Blasch, "Kalman Filtering with Nonlinear State Constraints," *IEEE Transaction on Aerospace and electronic Systems*, vol. 45, no. 1, pp. 70–84, 2009.
- [28] M. H. Afzal, V. Renaudin, and G. Lachapelle, "Magnetic field based heading estimation for pedestrian navigation environments," *2011 International Conference on Indoor Positioning and Indoor Navigation, IPIN 2011*, 2011.
- [29] S. Wang, H. Wen, R. Clark, and N. Trigoni, "Keyframe based Large-Scale Indoor Localisation using Geomagnetic Field and Motion Pattern," in *IEEE/RSJ International Conference on Intelligent Robots and Systems (IROS)*, pp. 1910–1917, 2016.
- [30] A. Markham and N. Trigoni, "Magneto-Inductive NETWORKED Rescue System (MINERS): Taking sensor networks underground," *2012 ACM/IEEE 11th International Conference on Information Processing in Sensor Networks (IPSN)*, pp. 1–11, 2012.
- [31] A. Markham, N. Trigoni, D. W. MacDonald, and S. A. Ellwood, "Underground localization in 3-D using magneto-inductive tracking," 2012.
- [32] D. D. Arumugam, "Decoupled range and orientation sensing in long-range magnetoquasistatic positioning," *IEEE Antennas and Wireless Propagation Letters*, vol. 14, no. 2, pp. 654–657, 2014.
- [33] D. D. Arumugam, "Single-Anchor 2-D Magnetoquasistatic Position Sensing for Short to Long Ranges above Ground," *IEEE Antennas and Wireless Propagation Letters*, vol. 15, no. 3, pp. 1325–1328, 2016.
- [34] D. Goshen-meskin and I. Y. Bar-itzhachkf, "Unified approach to inertial navigation system error modeling," *AIAA Journal of Guidance Control and Dynamics*, vol. 15, no. 3, pp. 648–653, 1992.
- [35] A. R. Jimenez, F. Seco, J. C. Prieto, and J. Guevara, "Indoor Pedestrian navigation using an INS/EKF framework for yaw drift reduction and a foot-mounted IMU," *Proceedings of the 2010 7th Workshop on Positioning, Navigation and Communication, WPNC'10*, pp. 135–143, 2010.
- [36] M. Ma, Q. Song, Y.-h. Li, Y. Gu, and Z.-m. Zhou, "A Heading Error Estimation Approach based on Improved Quasi-static Magnetic Field Detection," in *2016 International Conference on Indoor Positioning and Indoor Navigation (IPIN)*, 2016.
- [37] C. Xu, L. Zhang, L. Cheng, and R. Koch, "Pose Estimation from Line Correspondences: A Complete Analysis and A Series of Solutions," *IEEE Transactions on Pattern Analysis and Machine Intelligence*, no. 4, pp. 1–14, 2016.